Original Article

MOLECULAR METABOLISM

Autotaxin signaling facilitates β cell dedifferentiation and dysfunction induced by Sirtuin 3 deficiency

Huanyi Cao [1,2], Arthur C.K. Chung [1], Xing Ming [1,2], Dandan Mao [1,2], Heung Man Lee [1,2,3], Xiaoyun Cao [4], Guy A. Rutter [5,6,7], Juliana C.N. Chan [1,2,3], Xiao Yu Tian [4,**], Alice P.S. Kong [1,2,3,*]

ABSTRACT

Objective: β cell dedifferentiation may underlie the reversible reduction in pancreatic β cell mass and function in type 2 diabetes (T2D). We previously reported that β cell-specific *Sirt3* knockout (*Sirt3*f/f;Cre/+) mice developed impaired glucose tolerance and glucose-stimulated insulin secretion after feeding with high fat diet (HFD). RNA sequencing showed that *Sirt3*-deficient islets had enhanced expression of *Enpp2* (Autotaxin, or ATX), a secreted lysophospholipase which produces lysophosphatidic acid (LPA). Here, we hypothesized that activation of the ATX/LPA pathway contributed to pancreatic β cell dedifferentiation in *Sirt3*-deficient β cells.

Methods: We applied LPA, or lysophosphatidylcoline (LPC), the substrate of ATX for producing LPA, to MIN6 cell line and mouse islets with altered *Sirt3* expression to investigate the effect of LPA on β cell dedifferentiation and its underlying mechanisms. To examine the pathological effects of ATX/LPA pathway, we injected the β cell selective adeno-associated virus (AAV-*Atx*-shRNA) or negative control AAV-scramble in *Sirt3*f/f and *Sirt3*f/f;Cre/+ mice followed by 6-week of HFD feeding.

Results: In *Sirt3*f/f;Cre/+ mouse islets and *Sirt3* knockdown MIN6 cells, ATX upregulation led to increased LPC with increased production of LPA. The latter not only induced reversible dedifferentiation in MIN6 cells and mouse islets, but also reduced glucose-stimulated insulin secretion from islets. In MIN6 cells, LPA induced phosphorylation of JNK/p38 MAPK which was accompanied by β cell dedifferentiation. The latter was suppressed by inhibitors of LPA receptor, JNK, and p38 MAPK. Importantly, inhibiting ATX *in vivo* improved insulin secretion and reduced β cell dedifferentiation in HFD-fed *Sirt3*f/f;Cre/+ mice.

Conclusions: *Sirt3* prevents β cell dedifferentiation by inhibiting ATX expression and upregulation of LPA. These findings support a long-range signaling effect of *Sirt3* which modulates the ATX-LPA pathway to reverse β cell dysfunction associated with glucolipotoxicity.

© 2022 The Author(s). Published by Elsevier GmbH. This is an open access article under the CC BY-NC-ND license (http://creativecommons.org/licenses/by-nc-nd/4.0/).

Keywords Autotaxin; Lysophosphatidic acid; β cell dedifferentiation; Sirtuin3; Mitogen-activated protein kinases; Type 2 diabetes

1. INTRODUCTION

β cell failure and insulin resistance in peripheral tissues represent the core pathophysiologic defects in type 2 diabetes (T2D) [1]. Glucotoxicity, lipotoxicity, oxidative stress, endoplasmic reticulum stress, and inflammation are known factors which contribute to β cell dysfunction in T2D [2]. β cell dedifferentiation has emerged as a new player in β

cell failure, in addition to apoptosis or senescence, under metabolic stress in T2D [3]. Dedifferentiated β cells become progenitor-like cells or transdifferentiate into non-β pancreatic cells, such as α, δ, and polypeptide P (PP) cells with reduced β cell function and contribute to the progression of T2D [4]. During β cell dedifferentiation, marker genes vital for mature β cell function, such as β cell enriched genes (e.g. key transcription factors including *Foxo1, Pdx1, Nkx6.1*), glucose

[1]Department of Medicine and Therapeutics, The Chinese University of Hong Kong, Hong Kong SAR, China [2]Li Ka Shing Institute of Health Sciences, The Chinese University of Hong Kong, Hong Kong SAR, China [3]Hong Kong Institute of Diabetes and Obesity, The Chinese University of Hong Kong, Hong Kong SAR, China [4]School of Biomedical Sciences, The Chinese University of Hong Kong, Hong Kong SAR, China [5]CR-CHUM and Université de Montréal, Montréal, QC, Canada [6]Section of Cell Biology and Functional Genomics, Division of Diabetes, Endocrinology and Metabolism, Department of Metabolism, Digestion and Reproduction, Imperial College London, London, UK [7]Lee Kong Chian School of Medicine, Nanyang Technological University, Singapore

*Corresponding author. Department of Medicine and Therapeutics, The Chinese University of Hong Kong, Prince of Wales Hospital, Shatin, N.T., Hong Kong SAR, China. Fax: +(852) 2637 3852 E-mail: alicekong@cuhk.edu.hk (A.P.S. Kong).

**Co-corresponding author. School of Biomedical Sciences, The Chinese University of Hong Kong, Shatin, N.T., Hong Kong SAR, China. Fax: +(852) 2603 5123 E-mail: xytian@cuhk.edu.hk (X.Y. Tian).

metabolism genes (e.g. *Glut2, Idh2, Atp4a*), and protein secretory pathway genes (e.g. *Gipr, Trpm5, Btg2*), are downregulated. On the other hand, progenitor cell markers (e.g. *Ngn3, Aldh1a3, Sox9* and *Oct4*) and β cell "disallowed" genes (e.g. *Ldha, Slc16a1*) are upregulated [5—7].

Recent murine studies suggested the therapeutic potential of controlling β cell dedifferentiation as a strategy to improve β cell function [8,9]. Islets isolated from patients with T2D exhibited marked reduction in expression of SIRT3 protein [10]. *In vitro* studies confirmed reduced expression of both SIRT3 mRNA and protein in patients' islets exposed to high glucose condition [11]. On the other hand, overexpression of SIRT3 in rats islets alleviated palmitate-induced β cell dysfunction [12]. Consistent with these studies, we had reported reduced expression of SIRT3 protein in islets from adult male 129Sv mice after 8 weeks of HFD feeding. In *Sirt3* global knock-out mice, we revealed that *Sirt3* deficiency accelerated HFD-induced impairment of glucose homeostasis and β cell apoptosis. Islets from these mice also showed reduced glucose-stimulated insulin secretion (GSIS) [13].

To further elucidate the role of SIRT3 in the regulation of pancreatic β cells, our group has established the β cell-selective Sirtuin3 (*Sirt3*) knockout (*Sirt3*$^{f/f;Cre/+}$) mice by Ins2 Cre driven deletion of the *Sirt3* allele. After HFD feeding these *Sirt3*$^{f/f;Cre/+}$ mice exhibited a mixed phenotype including impaired glucose tolerance, reduced GSIS and increased hepatic steatosis [14]. Inhibiting 5-hydroxytryptamine synthesis in β cells from *Sirt3*$^{f/f;Cre/+}$ mice improved HFD-induced hepatic steatosis but failed to improve glucose tolerance [14]. These findings implicated alterative mechanisms in β cell dysfunction induced by *Sirt3* deficiency. RNA-sequencing of islets from *Sirt3*$^{f/f;Cre/+}$ mice led to discovery of 5-fold upregulation of Autotaxin (ATX, encoded by *Enpp2*) compared to those from *Sirt3*$^{f/f}$ animals, under both standard diet (STD) and HFD conditions.

ATX is a member of the ectonucleotide pyrophosphatase/phosphodiesterase (*Enpp*1-7) protein family. It is the only secreted enzyme in this family with its catalytically active form being detected in most biological fluids [15,16]. ATX, as a secreted lysophospholipase, is responsible to maintain the basal concentration of lysophosphatidic acid (LPA) in blood by hydrolyzing lysophosphatidylcholine (LPC) to LPA [17]. As an extracellular signaling molecule, LPA binds to six G protein coupled receptors namely LPAR1 to LPAR6. LPA is involved in various cellular processes including cell proliferation, survival, migration, differentiation, remodeling, and cytokine/chemokine secretion [18]. Dysregulation of ATX/LPA signaling is implicated in many diseases, including cancer, arthritis, pulmonary fibrosis and neurological disorders, as well as glucose homeostasis and obesity-related insulin resistance [19—23]. However, the mechanisms underpinning the association between ATX/LPA pathway and β cell function remain underexplored. In this study, we demonstrated that *Sirt3* deficiency in β cells induced β cell dysfunction by activating the ATX/LPA pathway to induce β cell dedifferentiation.

2. RESEARCH DESIGN AND METHODS

2.1. Cell culture, islet isolation and treatment

MIN6 pancreatic insulin-secreting cell line (passage from 20 to 30, kindly provided by Prof. Guang Ning, School of Medicine, Shanghai Jiao-Tong University, Shanghai, China) was cultured in a DMEM medium supplemented with 15% (vol./vol.) FBS, 100 U/ml penicillin, 0.1 mg/mL streptomycin and 110 μmol/L 2-mercaptoethanol (Invitrogen, USA). Pancreatic islets were isolated from the male *Sirt3*$^{f/f;Cre/+}$

and *Sirt3*$^{f/f}$ mice as previously described [13,14]. We applied 0.8 mg/mL Collagenase P (Roche, Switzerland) solution (around 3 mL), which was dissolved in Hanks' balanced salt solution HBSS (Invitrogen) for pancreas digestion. The HBSS and Histopaque 1119, 1083, and 1077 (Sigma—Aldrich) were applied for islets resuspension and isolation. The isolated islets were cultured in RPMI 1640 medium supplemented with 10% FBS and 100 U/ml penicillin, 0.1 mg/mL streptomycin (Invitrogen) for further treatment. 1- Oleoyl lysophosphatidic acid (LPA), ki16425 (LPA receptor inhibitor, or LPARi) were purchased from Cayman; SB203580 (p38 MAPK inhibitor, or p38 MAPKi), from R&D Systems; SP600125 (JNK1/2 inhibitor, or JNKi), from MedChemExpress; and L-α-Phosphatidylcholine (LPC), from Sigma—Aldrich.

2.2. shRNA lentivirus and adeno-associated virus establishment

We used published methods to knock down *Sirt3* expression in MIN6 cells [14]. For specific knockdown *Enpp2* expression in mouse pancreatic β cells, the Mus *Enpp2* shRNA plasmids were purchased from Sun Yuen Technology Limited (Hong Kong) and the shRNA construct sequences are as follows: shRNA- *Enpp2*-1: 5′-CCGGCGACCCAAGATTCCCAATAATCTCGAGATTATTGGGAATCTTGGGTCGTTTTTG -3′; shRNA-*Enpp2*-2: 5′-CCGGCCTGTACCAAATCTGACATATCTCGAGATATGTCAGATTTGGTACAGGTTTTTG -3′; shRNA *Enpp2*-3: 5′-CCGGGCCTTCAGTTTATGCCTTCTACTCGAGTAGAAGGCATAAACTGAAGGCTTTTTG -3′ and expressed scrambled negative shRNA: 5′-TTCTCCGAACGTGTCACGTTTCAAGAGAACGTGACACGTTCGGAGAATTTTTT -3′. In order to achieve selective ATX inhibition *in vivo*, we used recombinant AAV8 carrying *Atx*-shRNA driven by insulin 1 promoter for targeted delivery to mouse islets. PAV- insulin 1- RFP-mir30- m*Enpp2*-shRNA AAV8 (AAV-*Atx*-shRNA) and its scramble negative control were generated by ViGene. Male mice at 8 weeks of age were randomized to receive intraperitoneal injection with 1×10^{12} genome copies of AAV-*Atx*-shRNA or negative control AAV-scramble in 100 μL of normal saline.

2.3. Animal experiments, oral glucose tolerance test, and insulin tolerance test

Pancreatic β cell-selective *Sirt3* knockout (*Sirt3*$^{flox/flox}$; Ins-Cre$^{+/-}$ [herein named *Sirt3*$^{f/f;Cre/+}$]) mice and *Sirt3*$^{flox/flox}$ (herein named *Sirt3*$^{f/f}$) mice were generated as previously described [14]. The male *Sirt3*$^{f/f;Cre/+}$ and *Sirt3*$^{f/f}$ mice were fed with HFD (60% cal from fat; Research Diets D12492) at the age of 8 weeks and housed in pathogen-free conditions with a 12-h light—dark cycle. Body weight and food intake were measured every week, blood glucose levels were measured every 2 weeks between 9:00 and 10:00 am. Animal Experimental Ethics Committee of the Chinese University of Hong Kong approved the procedures (14/101/MIS and 19/184/MIS). Oral glucose tolerance tests (OGTT) and insulin tolerance tests (ITT) were conducted as previously described [14]. The glucose and insulin dosages were 2 g/kg and 0.75 IU/kg body weight, respectively. Insulin resistance was calculated as the area under the curve of glycemia (AUC; mg/dL*t) measured at 0, 30, 60 and 120 min after insulin administration, and glucose intolerance calculated as the AUC of the glycemia (mg/dL*t) measured at 0, 30, 60 and 120 min after glucose administration.

2.4. Glucose-stimulated insulin secretion (GSIS) and ELISA

Glucose-stimulated insulin secretion (GSIS) was measured as previously described [14]. ATX concentration in the conditioned medium and mouse serum was measured by ELISA from ImmunoDiagnostics; LPA concentration in the conditioned medium and mouse serum was
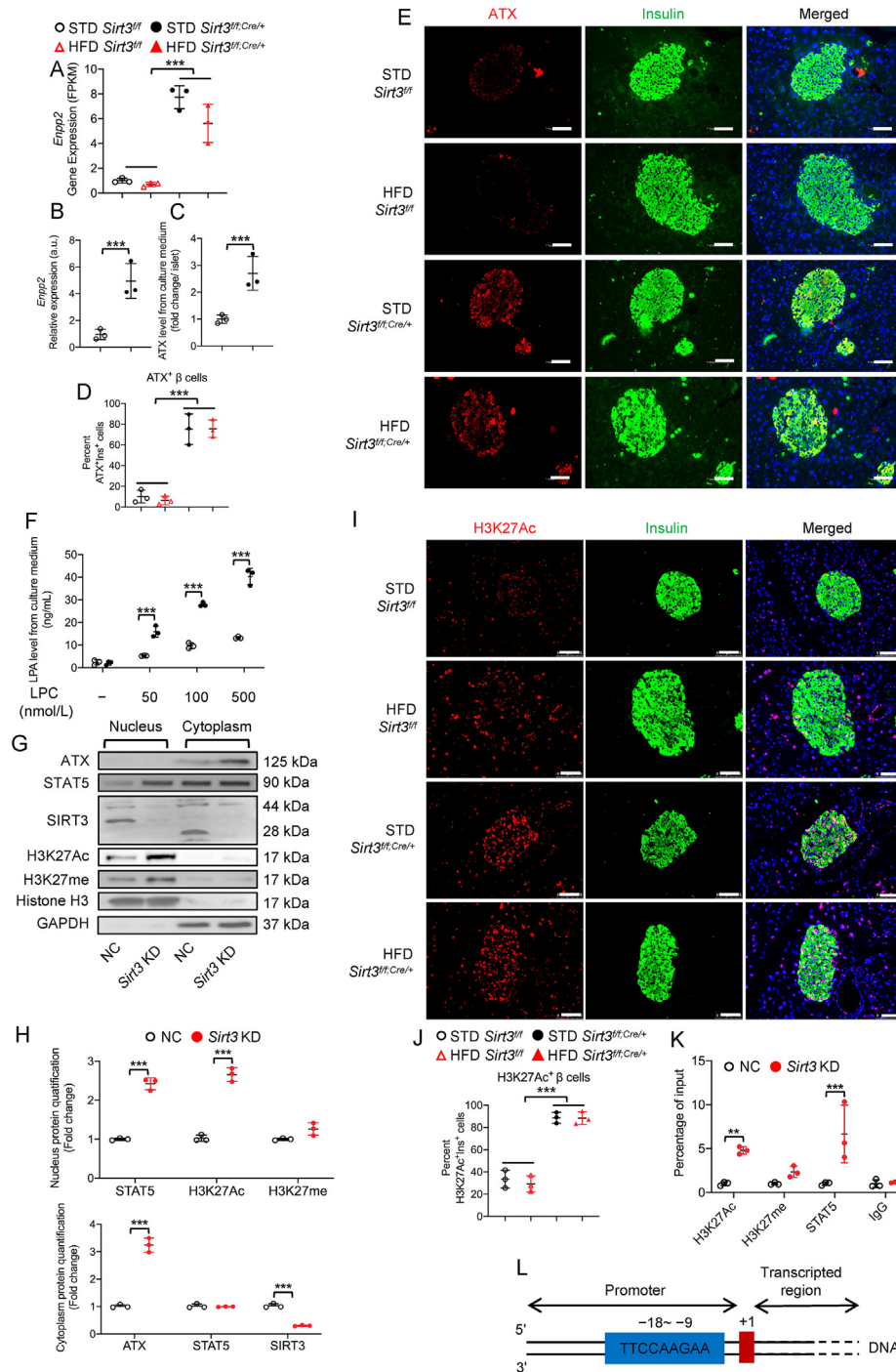
Figure 1: *Sirt3* **deficiency upregulated ATX expression in β cells**. *A*: The expression levels of *Enpp2* from RNA-Seq DEGs analysis (n = 3 mice per group). *B*: Relative mRNA expression level of *Enpp2* was assessed by RT-PCR in *Sirt3^f/f^* and *Sirt3^f/f;Cre/+^* mouse islets (n = 3 mice per group). *C*: ATX level measured in the culture medium from *Sirt3^f/f^* and *Sirt3^f/f;Cre/+^* mouse islets (n = 3 mice per group) *D*: Quantification of relative fluorescence positive areas shown in *E* (n = 3 mice per group, each containing 6−8 islets). *E*: Immunofluorescent staining of insulin and ATX in *Sirt3^f/f^* and *Sirt3^f/f;Cre/+^* mouse pancreas with STD or HFD feeding (scale bar, 50 μm, green: Insulin, red: ATX, blue: DAPI). *F*: LPA level measured in culture medium from *Sirt3^f/f^* and *Sirt3^f/f;Cre/+^* mouse islets in the presence of different concentrations of LPC (n = 3 mice per group). *HG*: Representative western immunoblot data of H3K27Ac, H3K27me and STAT5 from nucleus and cytoplasm of MIN6 cells after knockdown of *Sirt3*. Three independent experiments were repeated from different samples. *H*: Quantification of western immunoblot in *G*. *I*: Immunofluorescent staining of insulin and H3K27Ac in *Sirt3^f/f^* and *Sirt3^f/f;Cre/+^* mouse pancreas with STD or HFD feeding (scale bar, 50 μm, green: Insulin, red: H3K27Ac, blue: DAPI). *J*: Quantification of relative fluorescence positive areas shown in *I* (n = 3 mice per group, each containing 6−8 islets). *K*: Percentage of input in *Enpp2* promoter from immunoprecipitated DNA with antibody against H3K27Ac, H3K27me and STAT5 in MIN6 cells after knockdown of *Sirt3* were subjected to RT-PCR (n = 3 biological replicates). *L*: The base pair location of the *Enpp2* gene promoter being analyzed by ChIP. Data are presented as Mean ± SD. *, $P < 0.05$; **, $P < 0.01$; ***, $P < 0.001$ by Student *t* test. a.u., arbitrary units; ATX, autotaxin; STD, standard diet; HFD, high fat diet; NC, normal control; *Sirt3* KD, knockdown of *Sirt3*; H3K27Ac, acetyl- Lys 27 of histone H3; H3K27me, methylation of lysine 27 on histone H3; STAT5, signal transducer and activator of transcription 5; bp, base pairs. (For interpretation of the references to color in this figure legend, the reader is referred to the Web version of this article.)

measured by ELISA from MyBioSource; glucagon level in the mouse serum was measured by ELISA from Millipore; all according to the manufacturers' instructions.

2.5. Real time-PCR (RT-PCR) and immunoblotting

RT-PCR was performed with the SYBR Green kit (Promega) on Applied Biosystems 7900HT Fast Real-Time PCR System as previously described [14]. Data were normalized to *Gapdh* mRNA in each sample. Mouse primers sequences are shown in Supplementary Table. 1. Western immunoblot analysis was performed as previously described; protein (20—30 μg) was loaded into each well of 8—15% SDS-PAGE gel [14]. The protein used in Figure 1*G* was extracted and separated by nuclear and cytoplasmic, while the others were total extract. Primary antibodies are listed in Supplementary Table. 2. Horseradish peroxidase-linked anti-rabbit and anti-mouse IgG (1:2,000; Cell Signaling Technology) were used as secondary antibodies. Protein bands were developed by Immobilon Western Chemiluminescent HRP Substrate (Millipore).

2.6. Histological staining

We conducted tissue and cell immunofluorescence staining as previously described [13]. Rabbit anti H3K27Ac (1:200, Abcam, catalog #ab4729), PDX1 (1:1,000, Abcam, catalog, #ab47267), RFP (1:200, Thermo Fisher, catalog #PA1-986), ALDH1A3 (1:200, Proteintech, catalog #25167-1-AP), p-JNK (1:50, CST, catalog #4668), p-p38 MAPK (1:100, CST, catalog #4511), glucagon (1:200, Abcam, catalog #ab92517) and guinea pig anti-insulin (1:1,000, DAKO, catalog #A0564) and mouse anti-NKX6.1 (1:1,000, DSHB, catalog # F55A10), NGN3 (1:500, DSHB, catalog # F25A1B3) and ATX (1:200, Abcam, catalog, # ab77104) antibodies were applied to the sections overnight at 4 °C, followed by incubation with secondary antibodies (1:500). The images were captured by LEICA CTR6000, using the Leica Qwin image analysis software (Leica) and positive signals were quantified using Image J. Insulin positive cells, indicated by positive staining for β cell identity markers (NKX6.1 or PDX1) and H3K27Ac, were determined by counting the corresponding nuclear staining surrounding the insulin staining area. Quantification of NGN3 was performed in pancreatic sections double-stained for insulin and NGN3, by counting the number of NGN3 positive-insulin negative cells, within the islet area. The ALDH1A3, p-JNK and p-p38 MAPK positive cells were determined as ratio of insulin and these markers positive staining overlapping area expressed against total insulin positive area. Staining, photo acquirement and cell counting was done in a blinded manner and unblinding occurred after counting all samples.

2.7. Chromatin immunoprecipitation

Chromatin immunoprecipitation (ChIP) assays were carried out as previously described [14]. The first antibodies against H3K27Ac (Catalog #ab4729) and H3K27me (Catalog #ab6002) were from Abcam, STAT5 (Catalog #9363) and IgG were from Cell Signaling Technology. ChIP and input DNA was purified and analyzed by quantitative RT-PCR with primers (described in Supplementary Table. 3) directed to the *Enpp2* promoter.

2.8. Statistical analysis

Data are expressed as means ± SD. Differences between groups were analyzed by Student's *t* test or One-way ANOVA followed by Bonferroni post hoc test where appropriate. Statistical testing was performed using GraphPad Prism 8 software (GraphPad Software). Differences with *P* values of <0.05 were considered statistically significant for all tests.

3. RESULTS

3.1. *Sirt3* deficiency upregulated ATX expression in β cells

Sirt3$^{f/f;Cre/+}$ mice were generated and validated in our previous study [14]. RNA-sequencing indicated that *Enpp2* (*Atx*) was upregulated in islets after *Sirt3* deletion, as validated by RT-PCR, secreted ATX from islet into the culture medium, and immunostaining (Figure 1A—E), while the LPA receptors expression levels were not affected in islets (Supplementary Fig. 1A, B). The increased LPA level from culture medium in the presence of different concentrations of LPC was also observed in islets after *Sirt3* deletion (Fig. 1F). In view of the previous studies showing a direct regulatory role of SIRT3 in gene transcription by deacetylating histone markers [14,24,25], our previous study has demonstrated the binding of signal transducers and activators of transcription (STAT5) to both tryptophan hydroxylase 1 (*Tph1*) and *Tph2* promoters after *Sirt3* knockdown in MIN6 cells [14]. In current study, we measured the expression level of acetyl- Lys 27 of histone H3 (H3K27Ac) and methylation of lysine 27 on histone H3 (H3K27me) in MIN6 cells after knockdown of *Sirt3*. The results showed that knockdown of *Sirt3* increased H3K27Ac and STAT5 expression dramatically with a mild increase of H3K27me, which is in line with previous studies [14,25] (Figure 1G,H). The immunostaining results from mouse pancreases also confirmed that selective deletion of *Sirt3* in β cells was accompanied by upregulated expression of H3K27Ac in *Sirt3*$^{f/f;Cre/+}$ mice (Figure 1I,J). More importantly, the ChIP result showed that *Sirt3* knockdown was associated with enhancement of the binding of both H3K27Ac and STAT5 to the promoter region of the *Enpp2* genes, whereas involvement of H3K27me had minimal effect on the trans-activation of the *Enpp2* genes (Figure 1K and Supplementary Fig. 1C). Through Ensembl genome browser (https://asia.ensembl.org/), we also identified the binding motifs of STAT5 at the promoter regions of *Enpp2*. The STAT5 binding base pair location was from −18 to −9 in the *Enpp2* gene promoter which being analyzed by ChIP (Fig. 1L). These results suggested that SIRT3 might be involved in suppressing the activation histone marker H3K27Ac. Taken together, in the absence of SIRT3, increased acetylation of H3K27Ac might facilitate STAT5-induced transcription of ATX in β cell.

3.2. LPA induced β cell dedifferentiation

To examine the effect of LPA on β cell function, different concentrations of LPA were applied to MIN6 cells for 24 h. GSIS was more severely impaired by higher concentrations of LPA under high glucose treatment in MIN6 cells (Supplementary Fig. 2A), indicating that LPA impaired β cell function. LPA treatment (from 0.01 to 1 μmol/L) downregulated β cell identity genes, including *Foxo1, Nkx6.1, Pdx1* and *Neurod1*, whereas progenitor cell markers such as *Sox9* and *Oct4* were upregulated in MIN6 cells in a dose-dependent manner (Supplementary Fig. 2B, C).

To confirm the results obtained in MIN6 cells, GSIS was also studied in primary mouse islets treated with 0.1 μmol/L LPA or LPC, a concentration which did not impair β cell viability and induce apoptosis (Supplementary Fig. 2D-G). LPA, but not LPC, diminished the GSIS at 16.7 mmol/L glucose (Figure 2A). Similar to MIN6 cells, LPA, but not LPC, downregulated β cell identity genes, including *Foxo1, Nkx6.1* and *Pdx1*, while increased progenitor cell markers, *Aldh1a3, Ngn3, Sox9* and *Oct4*, as well as α cell enriched genes, such as *Arx* and *Mafb* in primary islets (Figure 2B,C). Western immunoblotting also demonstrated PDX1 and NKX6.1 downregulation, accompanied by increased expression of ALDH1A3, NGN3, and ARX after LPA treatment in MIN6 cells (Fig. 2D, E). Thus, these results showed that LPA
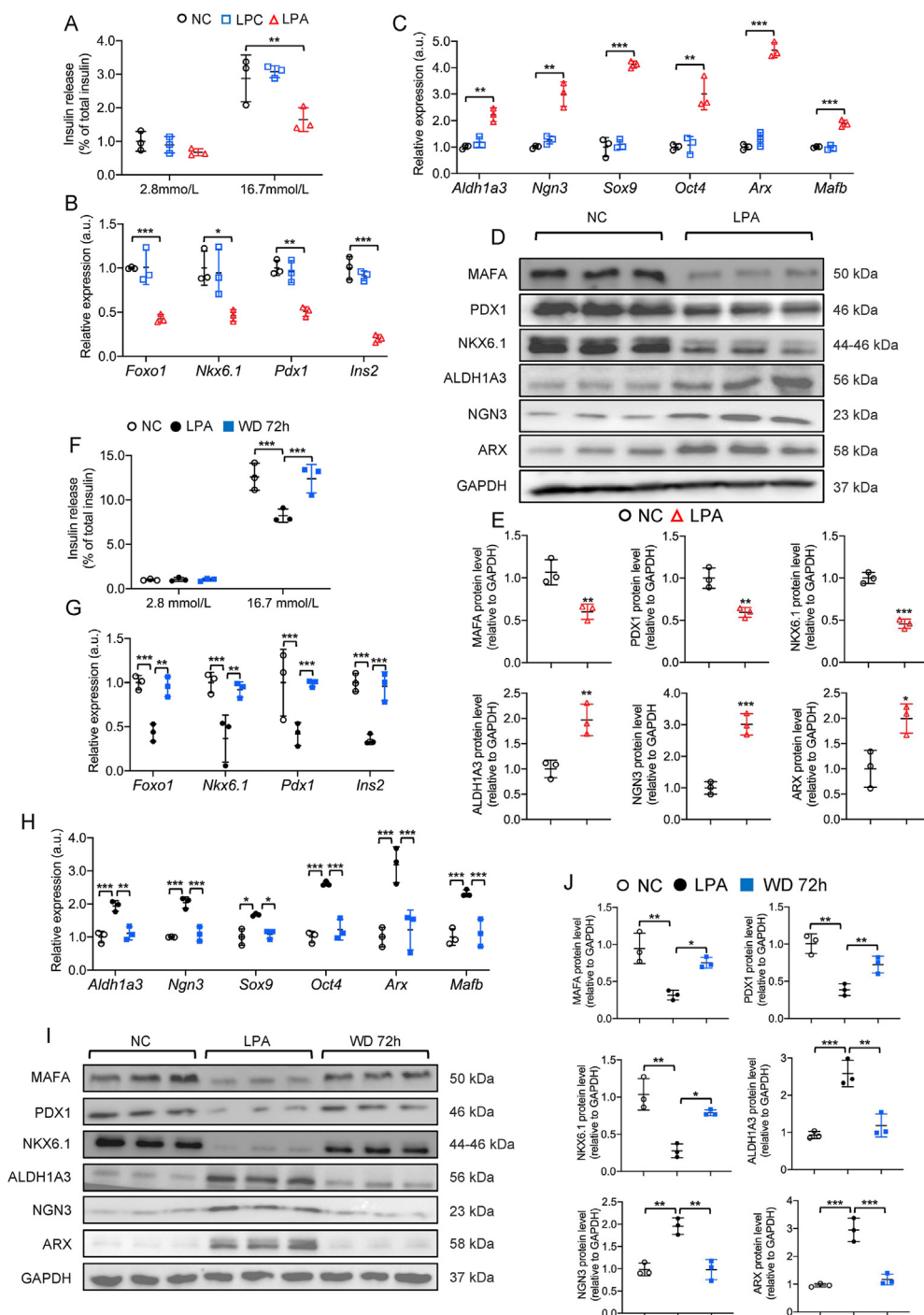
Figure 2: LPA induced β cell dedifferentiation. *A*: GSIS experiment was performed to evaluate β cell function with 0.1 μmol/L LPA treatment for 24 h in primary islets. *B*: Relative mRNA expression levels of β cell identity genes (including *Foxo1, Nkx6.1* and *Pdx1*) and *Ins2* were assessed by RT-PCR in primary islets with 0.1 μmol/L LPA or LPC treatment for 24 h. *C*: Relative mRNA expression levels of progenitor cell markers (*Aldh1a3, Ngn3, Sox9* and *Oct4*) and α cell enriched genes (such as *Arx* and *Mafb*) were assessed by RT-PCR in primary islets with 0.1 μmol/L LPA or LPC treatment for 24 h. *D*: Representative western immunoblot data (total protein) of β cell identity markers, progenitor cell markers and α cell enriched markers in MIN6 cells with 0.1 μmol/L LPA treatment for 24 h. *E*: Quantification of western immunoblot in *D*. *F*: Primary islets were treated with 0.1 μmol/L LPA for 24 h, followed by 72 h cultured with or without LPA treatment. GSIS was measured after different treatments. *G, H*: Primary islets were treated with 0.1 μmol/L LPA for 24 h, followed by 72 h cultured with or without LPA treatment. Relative mRNA expression levels of β cell identity genes (including *Foxo1, Nkx6.1* and *Pdx1*), *Ins2*, progenitor cell markers (*Aldh1a3, Ngn3, Sox9* and *Oct4*) and α cell enriched genes (such as *Arx* and *Mafb*) were assessed by RT-PCR after different treatments. *I*: MIN6 cells were treated with 0.1 μmol/L LPA for 24 h, followed by 72 h cultured with or without LPA treatment. Representative western immunoblot data (total protein) of β cell identity markers, progenitor cell markers and α cell enriched markers. *J*: Quantification of western immunoblot in *I*. Data are presented as Mean ± SD. *, $P < 0.05$; **, $P < 0.01$; ***, $P < 0.001$ by One-way ANOVA followed by Bonferroni post hoc test. n = 3 biological replicates. LPA, lysophosphatidic acid; LPC, lysophosphatidylcholine; *Foxo1*, forkhead box protein o 1; *Nkx6.1*, NK6 homeobox 1; *Pdx1*, pancreatic and duodenal homeobox 1; *Ins2*, insulin 2; *Aldh1a3*, aldehyde dehydrogenase 1a3; *Ngn3*, Neurogenin 3; *Sox9*, SRY-box transcription factor 9; *Oct4*, octamer-binding transcription factor 4; *Arx*, aristaless related homeobox; *Mafb*, MAF BZIP transcription factor b; MAFA, MAF BZIP transcription factor A; WD, withdrawing LPA treatment.

was able to trigger β cell dedifferentiation both in MIN6 cells and primary islets.

Others [26] have shown that, unlike apoptosis, β cell dedifferentiation can be reversed by a washout treatment to remove the stimuli. Accordingly, to determine the recovery of β cell function after withdrawing LPA treatment, GSIS analysis was performed. GSIS impaired by LPA was restored after withdrawing LPA (Fig. 2F). More importantly, the expression of β cell identity genes, progenitor cell markers, and α cell enriched genes were restored to their basal level after LPA was removed in both MIN6 cells and primary islets (Figure 2G—J and Supplementary Fig. 1H, I), suggesting the LPA induced β cell dedifferentiation could be reversed after LPA was removed.

3.3. *Sirt3* deficiency triggered LPC induced β cell dedifferentiation

To examine how SIRT3 modulated LPA-induced β cell dedifferentiation, knockdown *Sirt3* was performed in MIN6 cells by shRNA lentiviral infection (Figure 3A). The upregulation of *Enpp2* mRNA expression was observed in *Sirt3* knockdown (KD) MIN6 cells (Fig. 3A). Next, *Sirt3* KD and scrambled (NC) MIN6 cells were treated with the ATX substrate LPA or the ATX precursor LPC. After treatment, β cell identity genes *Nkx6.1, Pdx1*, and *Ins2* were similarly suppressed by LPA in both NC and *Sirt3* KD cells. In particular, LPC treatment suppressed these genes only in *Sirt3* KD cells, but not in NC cells (Fig. 3B). Likewise, LPA increased progenitor cell markers including *Ngn3* and *Oct4*, and α cell enriched genes *Arx* in both NC and *Sirt3* KD cells, while LPC only upregulated these genes in *Sirt3* KD cells (Fig. 3C). Furthermore, Western immunoblotting showed that LPC lowered PDX1 and NKX6.1 protein levels and upregulated ALDH1A3, NGN3, and ARX expression in *Sirt3* KD cells, but not NC controls (Figure 3D and Supplementary Fig. 2). These results suggested that the effect of LPC to induce β cell dedifferentiation was dependent on SIRT3 expression, supporting our hypothesis that SIRT3 modulated the ATX expression to facilitate LPC conversion to LPA.

We further validated the different effects of LPA and LPC obtained from MIN6 cells in mouse primary islet isolated from *Sirt3^f/f^* and *Sirt3^f/f;Cre/+^* mice. Two β cell identity markers, NKX6.1 and PDX1 were examined by immunofluorescence of the islet treated with LPA or LPC. We found that similar to MIN6 cells, LPA induced downregulation of both NKX6.1 and PDX1 in mouse islet of both groups, while LPC suppressed NKX6.1 and PDX1 only in islet from *Sirt3^f/f;Cre/+^* mice (Figure 3E,F and H, I). Conversely, the expression of progenitor cell marker ALDH1A3 was upregulated by LPA in both *Sirt3^f/f^* and *Sirt3^f/f;Cre/+^* mouse primary islets, but upregulated by LPC only in *Sirt3^f/f;Cre/+^* islets (Figure 3G,J). Collectively, the result from islets also showed that LPC induced β cell dedifferentiation in *Sirt3* deficient β cells.

3.4. JNK/p38 MAPK signaling pathways contributed to LPA induced β cell dedifferentiation

Although previous studies examined the effects of LPA in kidney, liver, and other tissues [27], the underlying mechanism of LPA-induced β cell dedifferentiation was still unclear. Earlier works from *in vitro* cell culture experiments suggested the Mitogen-Activated Protein Kinases (MAPKs) might be involved in the effect of LPA in different cells, like neuronal PC12 cells and ovarian theca cells. In addition, in β cells, there was negative correlation between β cell function and the activity levels of JNK1/2 and p38 MAPK [28]. Based on this evidence, we further examined whether JNK1/2 and p38 MAPK signaling were the downstream effectors of LPA signaling in β cells. In MIN6 cells, LPA increased the phosphorylation of JNK1/2 and p38 MAPK which peaked at 2 h in MIN6 cells (Figure 4A,B). Similar to the results for β cell dedifferentiation markers, LPC also increased the phosphorylation of

JNK1/2 and p38 MAPK only in *Sirt3* KD MIN6 cells (Figure 4C,D). These results suggested that LPA could activate the JNK and p38 MAPK, whereas the activating effect of LPC on these two signals was dependent on the loss of *Sirt3*, and most likely via ATX expression. We tested whether the effect of LPA could be blocked by the selective dual LPA receptor 1/3 inhibitor (LPARi), ki16425. LPARi treatment dose-dependently decreased LPA-induced phosphorylation of JNK1/2 and p38 MAPK in MIN6 cells (Figure 4E,F and Supplementary Fig. A-C). At a concentration of 10 μmol/L, LPARi showed effective inhibition and the dose was used in other experiments. As expected, 10 μmol/L LPARi abolished LPA-induced β cell dedifferentiation (Figure 4G,H).

Next, we used SP600125 as a JNK1/2 inhibitor (JNKi), and SB203580 as a p38 MAPK inhibitor (p38 MAPKi) to examine whether suppression of these signaling pathways would attenuate the effect of LPA on dedifferentiation in MIN6 cells. We found that both JNK and p38 MAPK inhibitors abolished LPA-induced downregulation of PDX1, and NKX6.1. In addition, the combination of both inhibitors showed better recovery of PDX1 and NKX6.1 expression. Regarding the progenitor markers, p38 MAPKi showed slightly more inhibition on ALDH1A3 and ARX upregulation. Similar to the effect on β cell identity markers, the combination of JNK and p38 MAPK inhibitors showed more inhibition on ALDH1A3, ARX, and NGN3 upregulation in MIN6 cells induced by LPA (Figure 4I,J). The mRNA expression levels of other markers (*Ins2, Sox9, Oct4 and Mafb*) further corroborated the above findings (Figure 4K,L). In *Sirt3* KD cells, inhibiting JNK and p38 MAPK abolished the β cell dedifferentiation induced by LPC (Figure 4M,N and Supplementary Fig. 4D-G). Taken together, these results indicated that both JNK and p38 MAPK signaling were downstream effectors of ATX-LPA signaling on β cell dedifferentiation.

3.5. Specific knockdown ATX improved HFD-induced glucose intolerance in *Sirt3^f/f;Cre/+^* islets in mice

Then we suspected selective suppression of ATX expression in pancreatic β cells might relieve the HFD-induced glucose intolerance in mice, especially when islet expression of *Sirt3* was reduced. In order to achieve selective ATX inhibition *in vivo*, we used recombinant AAV8 [29] carrying *Atx*-shRNA driven by insulin 1 promoter for specifically suppressing ATX expression in mouse islets of normal mice and mice with islet specific deletion of *Sirt3*. After injection of the 1×10^{12} genome copies per mouse of AAV-*Atx*-shRNA or negative control AAV-scramble in the *Sirt3^f/f^* and *Sirt3^f/f;Cre/+^* mice at 8 weeks, the mice were fed a HFD for 6 weeks for further investigation of whether selective knocking down of ATX in pancreatic β cells might ameliorate HFD-induced glucose intolerance in *Sirt3^f/f;Cre/+^* mice (Figure 5A).

Six weeks after HFD feeding, mice with both genotypes underwent OGTT and ITT tests. The HFD-induced glucose intolerance was attenuated after AAV-*Atx*-shRNA injection (Figure 5B,C). Serum insulin levels measured in mouse serum collected during OGTT indicated that knockdown of ATX expression in *Sirt3^f/f;Cre/+^* mouse β cells rescued insulin secretion impaired by HFD (Figure 5D,E). Although the lower fasting serum insulin level of the HFD fed *Sirt3^f/f;Cre/+^* mice was augmented after AAV-*Atx*-shRNA injection, there was no difference of insulin sensitivity, fasting serum glucagon level, fasting blood glucose (FBG), body weight and food intake among these mice after AAV-*Atx*-shRNA injection (Supplementary Fig. 5 A-G). Then, we validated the efficiency and specificity of ATX knockdown in mouse pancreatic β cells (Supplementary Fig. 5 and Supplementary Fig. 6H, I). As expected, ATX protein expression was effectively suppressed in HFD-fed *Sirt3^f/f;Cre/+^* mice by AAV-*Atx*-shRNA. These results also demonstrated that the co-localization between ATX and insulin, not
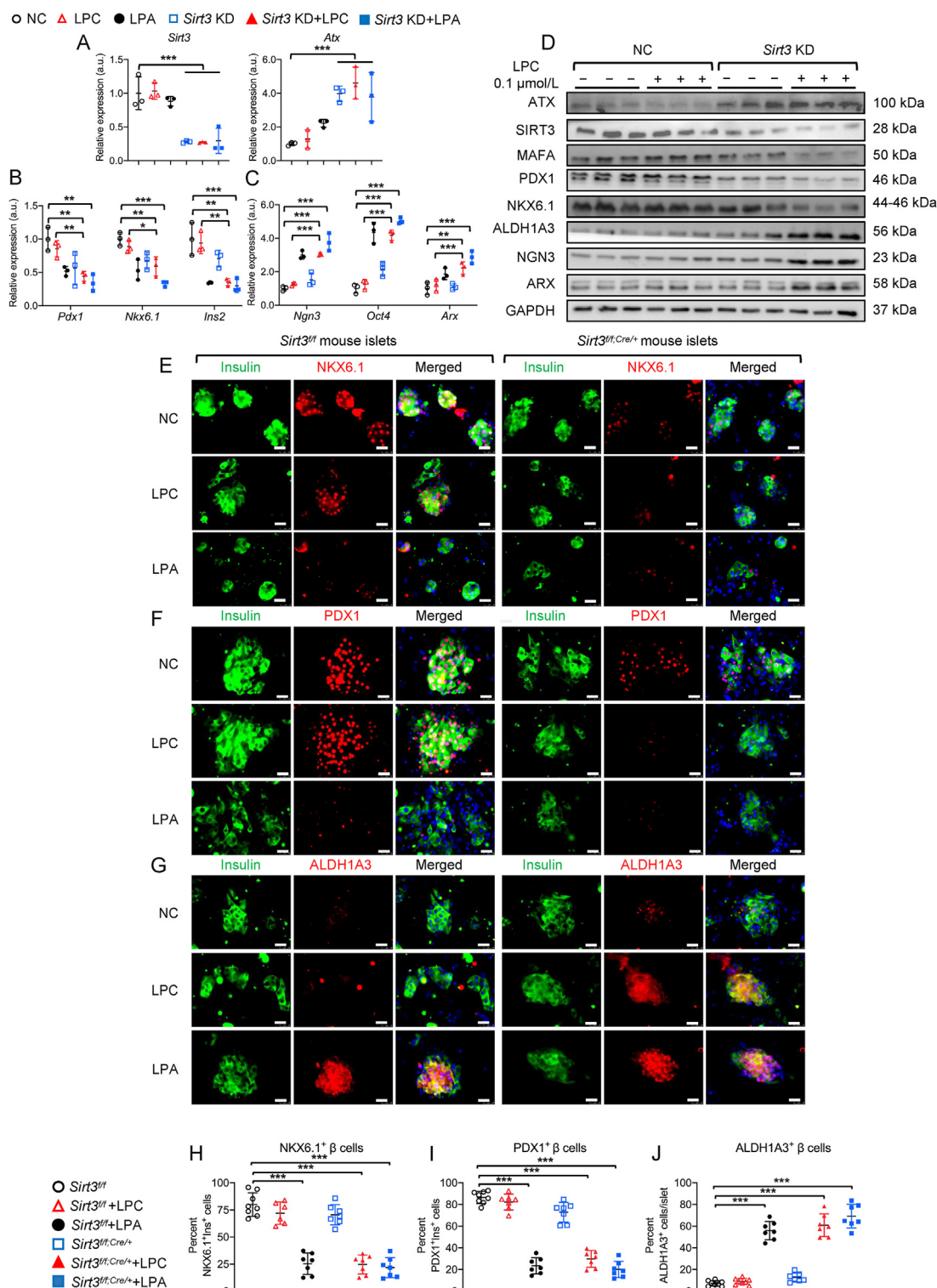
Figure 3: *Sirt3* deficiency triggered LPC induced β cell dedifferentiation. *A*: Relative mRNA expression levels of *Sirt3* and *Atx* were assessed by RT-PCR in MIN6 cells after knockdown of *Sirt3*; *B, C*: Relative mRNA expression levels of β cell identity genes, *Ins2*, progenitor cell markers and α cell enriched genes were measured by RT-PCR in normal and *Sirt3* deficiency MIN6 cells after treatment with 0.1 μmol/L LPA or LPC. *D*: Representative western immunoblot data (total protein) of SIRT3, ATX, β cell identity markers, progenitor cell markers and α cell enriched markers in normal and *Sirt3* deficiency MIN6 cells with 0.1 μmol/L LPC treatment for 24 h (n = 3 biological replicates). *E-G*: Immunocytochemistry of NKX6.1 (*E*), PDX1 (*F*) and ALDH1A3 (*G*) in primary islets isolated from *Sirt3^{f/f}* and *Sirt3^{f/f;Cre/+}* mice with 0.1 μmol/L LPC or LPA treatment for 24 h (scale bar, 25 μm). Green, Insulin; red, NKX6.1 (*E*), PDX1 (*F*) and ALDH1A3 (*G*); blue, Hoechst. *H-J*: Quantification of relative fluorescence positive areas shown in *E-G* (n = 6−8 islets). Data are presented as Mean ± SD. *, *P* < 0.05; **, *P* < 0.01; ***, *P* < 0.001 by One-way ANOVA followed by Bonferroni post hoc test. (For interpretation of the references to color in this figure legend, the reader is referred to the Web version of this article.)
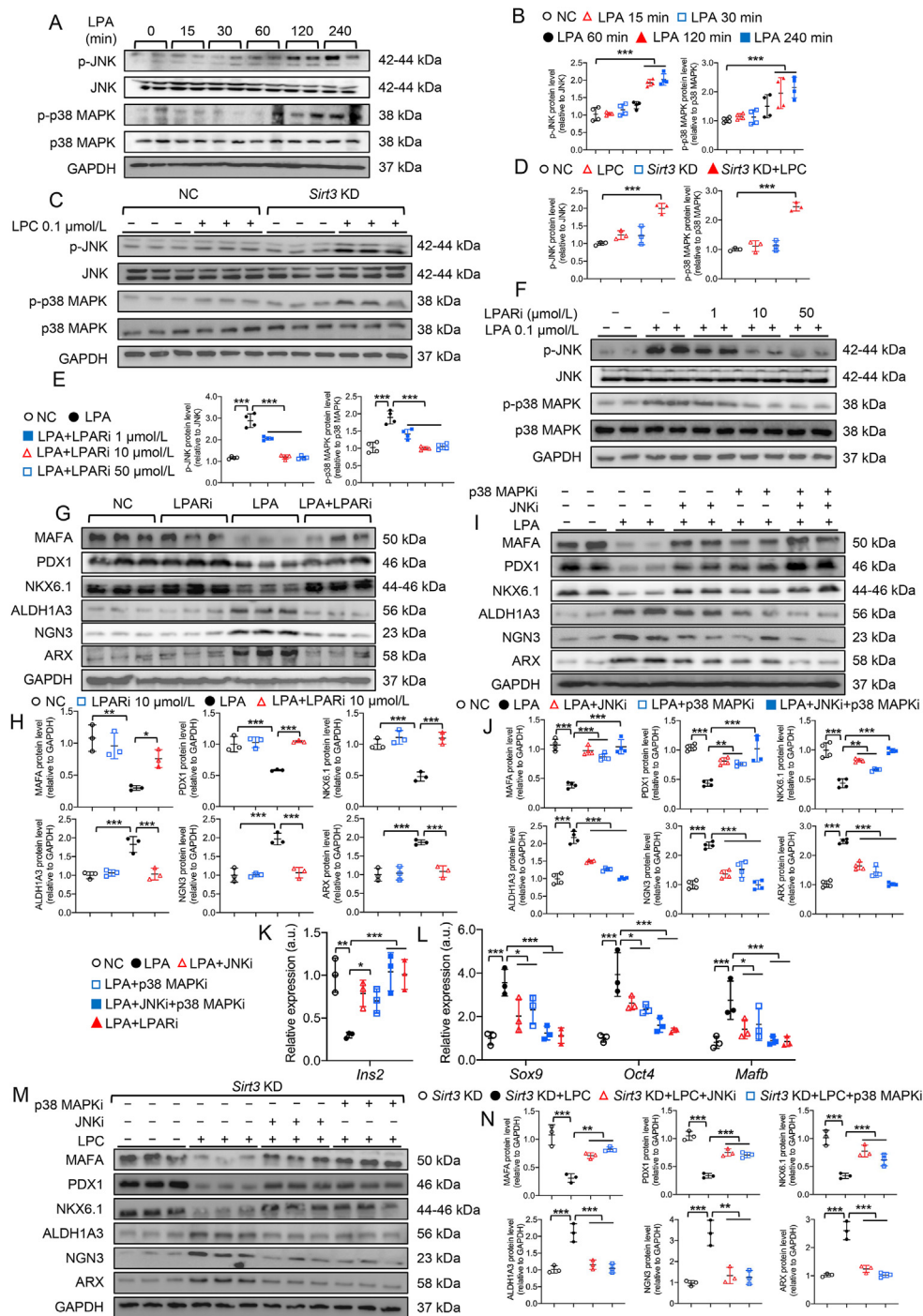
Figure 4: JNK/p38 MAPK signaling pathways contributed to LPA induced β cell dedifferentiation. *A*: Representative western immunoblot data (total protein) of p-JNK (Thr183/Tyr185)/JNK and p-p38 MAPK (Thr180/Tyr182)/p38 MAPK in MIN6 cells with 0.1 μmol/L LPA treatment for different timepoints. *B*: Quantification of western immunoblot in *A*. *BC*: Representative western immunoblot data (total protein) of p-JNK (Thr183/Tyr185)/JNK and p-p38 MAPK (Thr180/Tyr182)/p38 MAPK in normal and *Sirt3* KD MIN6 cells with 0.1 μmol/L LPC treatment for 2 h. *D*: Quantification of western immunoblot in *C*. *E*: Quantification of western immunoblot in *F*. *F*: Representative western immunoblot data (total protein) of p-JNK (Thr183/Tyr185)/JNK and p-p38 MAPK (Thr180/Tyr182)/p38 MAPK in LPA treated MIN6 cells after treatment with different concentrations of LPAR inhibitor. *G*: Representative western immunoblot data (total protein) of β cell identity markers, progenitor cell markers and α cell enriched markers in MIN6 cells with different treatments. *H*: Quantification of western immunoblot in *G*. *I*: Representative western immunoblot data (total protein) of β cell identity markers, progenitor cell markers and α cell enriched markers in MIN6 cells with different treatments. *J*: Quantification of western immunoblot in *I*. *K, L*: Relative mRNA expression levels of *Ins2*, progenitor cell markers (*Sox9* and *Oct4*) and α cell enriched genes (such as *Mafb*) were assessed by RT-PCR after different treatments. *M*: Representative western immunoblot data (total protein) of β cell identity markers, progenitor cell markers and α cell enriched markers in *Sirt3* KD MIN6 cells with different treatments. *N*: Quantification of western immunoblot in *M*. Data are presented as Mean ± SD. *, $P < 0.05$; **, $P < 0.01$; ***, $P < 0.001$ by One-way ANOVA followed by Bonferroni post hoc test. n = 3 biological replicates in Figure 4C,D, G, H and K-N. n = 4 biological replicates in Figure 4A,B, E, F, I, J. JNK1/2, c-jun N- Terminal Kinases; p38 MAPK, p38- Mitogen Activated Protein Kinase; LPARi, LPA receptor inhibitor, JNKi, JNK1/2 inhibitor; p38 MAPKi, p38 MAPK inhibitor.
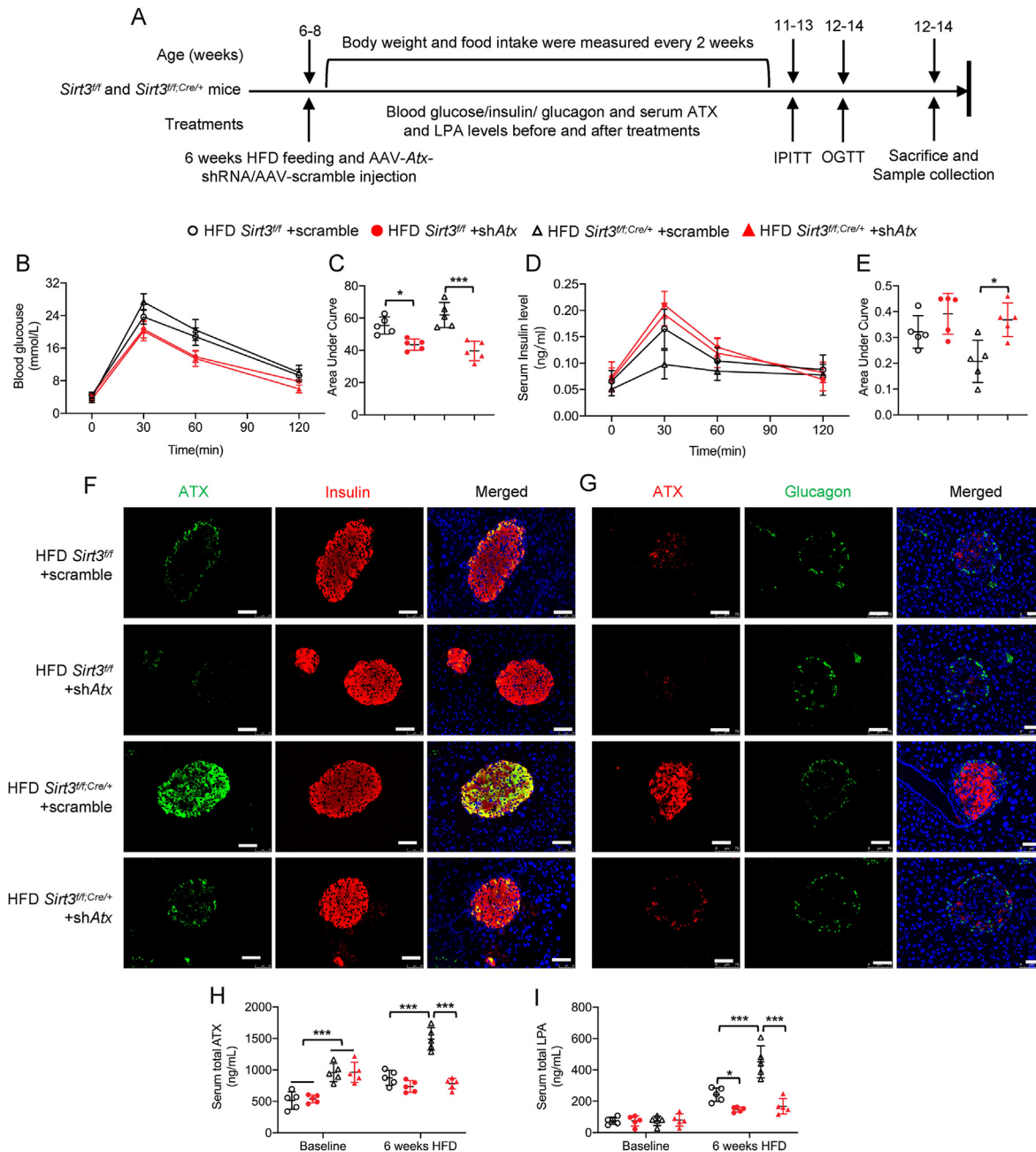
Figure 5: Specific knockdown ATX improved HFD-induced glucose intolerance in *Sirt3*^*f/f;Cre/+*^ islets in mice. *Sirt3*^*f/f*^ and *Sirt3*^*f/f;Cre/+*^ mice were injected with AAV-*Atx*-shRNA (for specific knocking down ATX in pancreatic β cells) or AAV-scramble respectively followed by HFD feeding for 6 weeks before sacrifice. *A*: Experimental design of 6 weeks' HFD feeding, AAV-*Atx*-shRNA injection and other experiments conducted on *Sirt3*^*f/f*^ and *Sirt3*^*f/f;Cre/+*^ mice (n = 5 per group). *B, C*: OGTT was performed before sacrifice and related AUC was calculated (n = 5 mice per group). *D, E*: During OGTT, blood samples were collected at each time point, serum was extracted from blood samples for insulin level measurement and related AUC was calculated (n = 5 mice per group). *F, G*: Immunostaining of insulin and ATX in mouse pancreas (scale bar, 50 μm). For immunofluorescent staining, *F*: green, ATX; red, insulin; blue, DAPI; *G*: green, glucagon; red, ATX; blue, DAPI. *H, I*: Serum ATX and total LPA levels were measured (n = 5 mice per group). *, *P* < 0.05; **, *P* < 0.01; ***, *P* < 0.001 by One-way ANOVA followed by Bonferroni post hoc test. AAV, Adeno-associated viruses; OGTT, oral glucose tolerance test; AUC, Area under curve. (For interpretation of the references to color in this figure legend, the reader is referred to the Web version of this article.)

glucagon, in *Sirt3*^*f/f;Cre/+*^ mouse islets (Figure 5F,G). Compared to the baseline, which collected before any treatments, serum ATX and total LPA level were also decreased after 6 weeks HFD feeding with AAV-*Atx*-shRNA injection (Figure 5H,I). These results implicated that selective suppression of ATX expression in pancreatic β cells rescued the HFD-induced glucose intolerance and restored insulin secretion in *Sirt3*^*f/f;Cre/+*^ islets in mice.

3.6. Specific knockdown ATX improved HFD-induced β cell dedifferentiation in *Sirt3*^*f/f;Cre/+*^ islets in mice

We then examined the molecular effects of ATX/LPA pathway in β cell dedifferentiation *in vivo*. Consistent with the *in vitro* results, selective knockdown of ATX in pancreatic β cells attenuated HFD-induced activation of JNK/p38 MAPK signal in *Sirt3*^*f/f;Cre/+*^ mice (Figure 6A,B and Supplementary Fig. 5J, K). The results showed that β cell identity
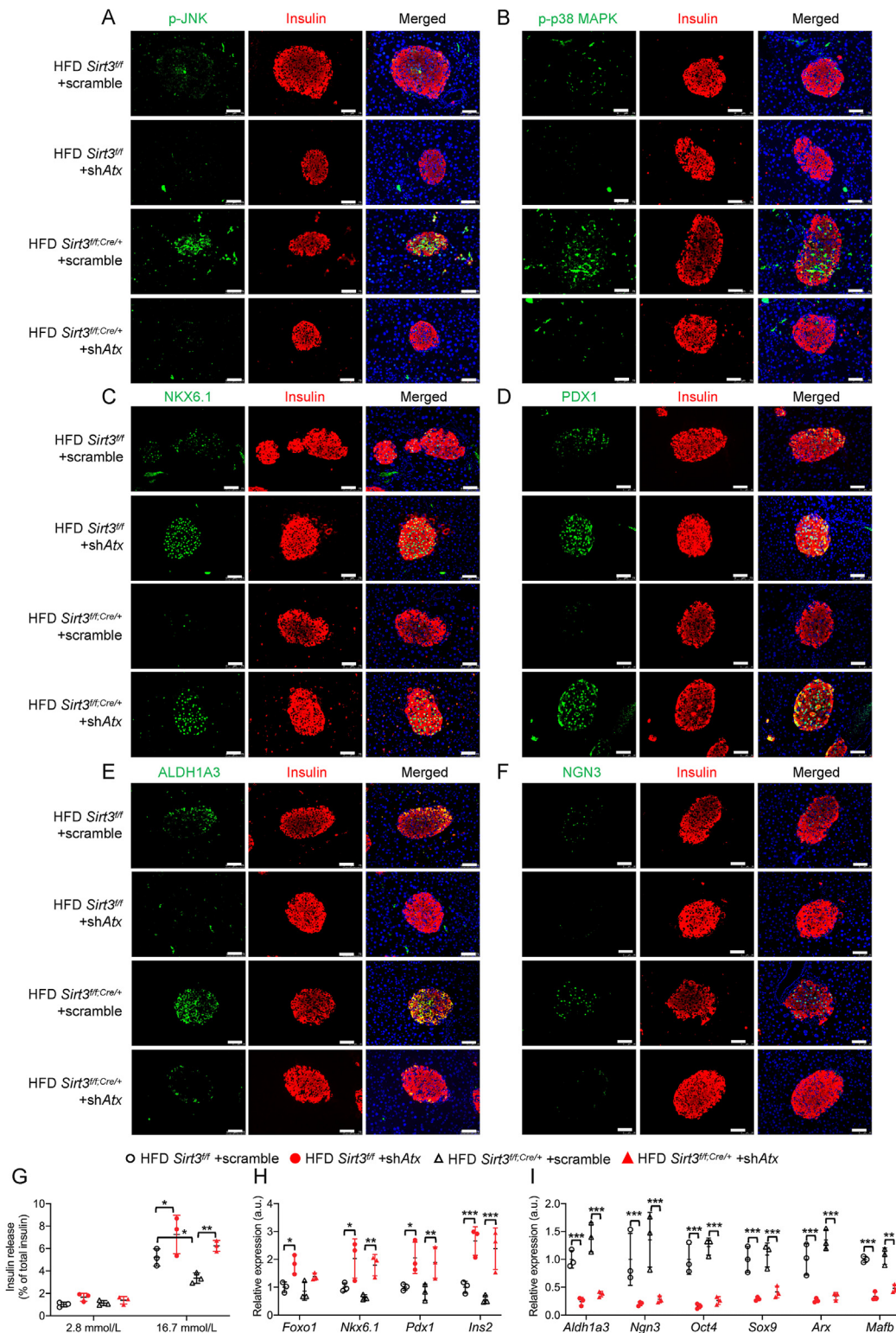
Figure 6: Specific knockdown ATX improved HFD-induced β cell dedifferentiation in *Sirt3$^{f/f;Cre/+}$* islets in mice. *Sirt3$^{f/f}$* and *Sirt3$^{f/f;Cre/+}$* mice were injected with AAV-*Atx*-shRNA (for specific knocking down ATX in pancreatic β cells) or AAV-scramble respectively, followed by feeding with HFD for 6 weeks before sacrifice. A-F: Immunofluorescent staining of insulin and JNK/p38 MAPK pathway or β cell dedifferentiation markers in mouse pancreas (scale bar, 50 μm). Green, p-JNK (*A*), p-p38 MAPK (*B*), NKX6.1 (*C*), PDX1 (*D*), ALDH1A3 (*E*) and NGN3 (*F*); red, insulin; blue, DAPI. *G*: GSIS was measured in isolated primary islets from four groups of mice (n = 3 mice per group). *H, I*: Relative mRNA expression levels of β cell identity genes (including *Foxo1, Nkx6.1* and *Pdx1*), *Ins2*, progenitor cell markers (*Aldh1a3, Ngn3, Sox9* and *Oct4*) and α cell enriched genes (such as *Arx* and *Mafb*) were assessed by RT-PCR in isolated primary islets from four groups of mice (n = 3 mice per group). Data are presented as Mean ± SD. *, $P < 0.05$; **, $P < 0.01$; ***, $P < 0.001$ by One-way ANOVA followed by Bonferroni post hoc test. (For interpretation of the references to color in this figure legend, the reader is referred to the Web version of this article.)
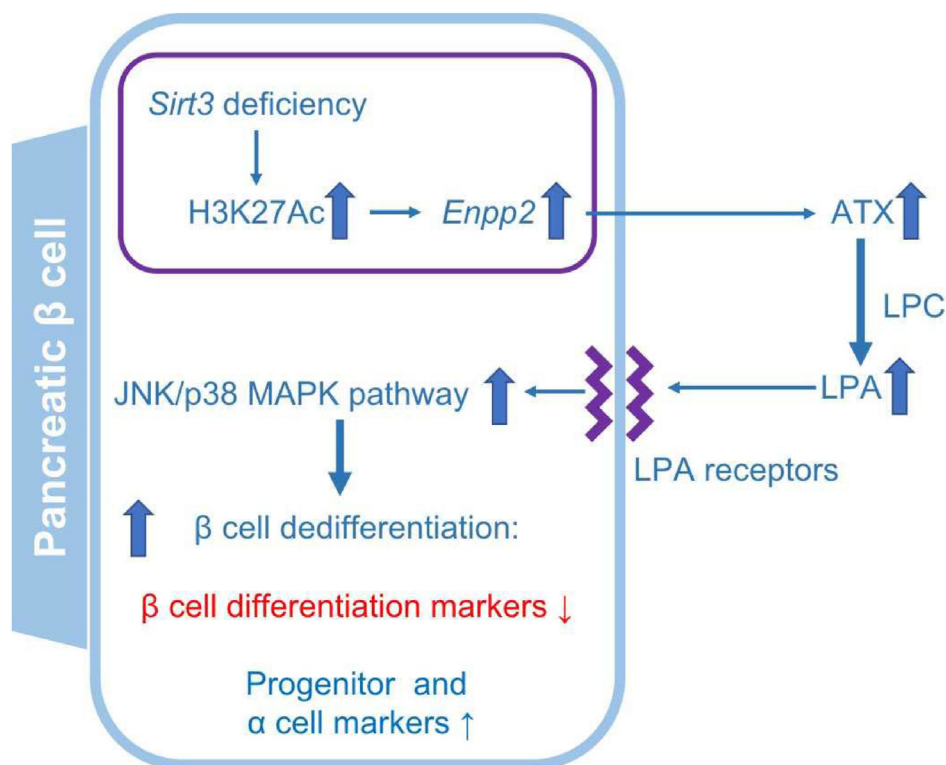
Figure 7: Proposed mechanisms linking *Sirt3*-ATX/LPA pathway and pancreatic β cell dedifferentiation.

markers, NKX6.1 and PDX1, which was downregulated in *Sirt3^f/f^* and *Sirt3^f/f;Cre/+^* mice, significantly increased after AAV-*Atx*-shRNA treatment (Figure 6C,D and Supplementary Fig. 5 L, M). Likewise, the expression of ALDH1A3 and NGN3, as the progenitor cell markers, which was increased in the *Sirt3^f/f^* and *Sirt3^f/f;Cre/+^* mice upon HFD feeding, was suppressed by AAV-*Atx*-shRNA (Figure 6E,F and Supplementary Fig. 5N, O). Furthermore, GSIS experiment on isolated islets showed AAV-*Atx*-shRNA improved insulin secretion in islets from both genotypes (Fig. 6G). Profiling of the mRNA expression in isolated islets also showed that similar to immunostaining, the downregulation of β cell identity genes (*Foxo1, Nkx6.1* and *Pdx1*) in *Sirt3^f/f;Cre/+^* mice was improved by AAV-*Atx*-shRNA, whereas the upregulation of progenitor cell markers (*Aldh1a3, Ngn3, Sox9* and *Oct4*) and α cell enriched genes, (*Arx* and *Mafb*) in *Sirt3^f/f;Cre/+^* mice was suppressed by AAV-*Atx*-shRNA (Figure 6H,I). These results suggested that inhibiting ATX suppressed HFD-induced β cell dedifferentiation in *Sirt3^f/f;Cre/+^* islets in mice. These results confirmed the pathological role of ATX in β cell dedifferentiation *in vivo.*

4. DISCUSSION

Accumulating evidence suggests that the loss of β cell identity and dedifferentiation is one of the primary processes responsible for impaired β cell function in T2D [4,30]. In the present study, we again demonstrated that *Sirt3* expression played a critical role in maintaining normal β cell function. Reduction or absence of *Sirt3* expression in β cells induced β cell dysfunction and glucose intolerance in mice. To our best knowledge, this is the first report showing that reduction or absence of *Sirt3* expression induced β cell dedifferentiation by activating the ATX/LPA pathway to cause β cell dysfunction (Figure 7).

Like its family members, *Sirt3* is classified as a deacetylase. Scher MB et al. first demonstrated that the full-length SIRT3 protein was enzymatically active and deacetylated acetyl-Lys 9 of histone H3 (H3K9Ac) and acetyl-Lys 16 of histone H4 (H4K16Ac) *in vivo* and *in vitro* [24]. SIRT3 had been shown to inhibit FOS transcription through specific histone H3 lysine K27 deacetylation (H3K27Ac) at its promoter to prevent inflammation and fibrosis in the mouse heart [31]. *Sirt3* knockout or *Sirt3* silencing by siRNA increased the acetylation level of H3K27Ac to promote the transcription of target proteins in primary brown adipocytes [25]. Interestingly, increased transcription at the *ENPP2* locus was related to the changes in expression of H3K27me in HEK 293T cell [32]. Similar with these studies, we had reported that knockdown of *Sirt3* increased H3K9Ac and H4K16Ac with binding of H4K16Ac, CREBP, and STAT5 to the promoter regions of the *Tph1* and *Tph2* genes by ChIP in sh-*Sirt3* MIN6 cells [14]. Collectively, these studies suggested that SIRT3 protein might function as deacetylase of histone and other nuclear proteins in addition to its major role as protein deacetylase in the mitochondria. In our current study, we found that knockdown of *Sirt3* increased acetylation of H3K27Ac and binding of STAT5 to the promoter regions of the ATX genes. Taken together, these results suggested that SIRT3 protein might modulate ATX levels via its deacetylase activity to activate ATX/LPA pathway to induce β cell dysfunction.

On the other hand, the key feature of mature β cell is to produce and secret insulin for maintaining glucose homeostasis [33]. Under physiological conditions, increased blood glucose stimulates insulin secretion in mature β cells to maintain blood glucose within a narrow range without causing hypoglycemia [34]. The characteristics of the mature functional β cell include: high expression of β cell identity genes, as well as low or no expression of progenitor cell marker genes, disallowed genes, and α cell enriched genes. Over-expression of these genes could interfere with normal β cell function [35]. Here, we

showed that LPA was able to suppress GSIS in primary islets and MIN6 cells. Increased LPA levels also induced β cell dedifferentiation in MIN6 cells and primary islets by downregulating expression of β cell identity genes (*Foxo1, Nkx6.1* and *Pdx1*), and concomitantly upregulating expression levels of progenitor cell markers (*Aldh1a3, Ngn3, Sox9* and *Oct4*) and α cell enriched genes (*Arx* and *Mafb*). Interestingly, after withdrawal of LPA, dedifferentiated β cells could redifferentiate to mature insulin positive β cells upon normalization of glucose levels, similar to previous studies using cell lineage tracing [36]. Clinical studies also supported potential reversibility of β cell dedifferentiation process with recovery of β cell function after removal of metabolic stress [37,38] such as hyperlipidemia and insulin resistance.

Several lines of evidence implicated *in vitro* activation of ATX could lead to increased LPA synthesis with the majority being extracellular [39,40]. Pharmacological inhibitors of ATX, such as PF8380, decreased plasma LPA levels to more than 95% [41]. Other researchers had also reported involvement of the ATX/LPA pathway in various metabolic disorders including obesity and insulin resistance [40,42]. In obese patients with insulin resistance and glucose intolerance, mRNA abundance of *Atx* in adipose tissue and circulating ATX levels were higher than controls with normal glucose tolerance [43,44]. Notably, despite taking obesogenic diet which induced glucose intolerance, insulin resistance was alleviated in both global heterozygous ATX deficient mice and adipose-specific ATX deficient mice [39,40,45]. Moreover, HFD feeding to the ATX-overexpressing mice showed bigger increment in body weight and adiposity than the control [40] although the underlying mechanism remains to be explored.

In another experiment using C57/BL6 mice fed with normal diet and high fat high sucrose (HFHS) diet, a single intraperitoneal injection of LPA caused impaired glucose tolerance more so in the HFHS-fed diet. These acute systemic effects of LPA could be attenuated by pre-injection with a dual LPAR 1/3 antagonist (ki16425). Importantly, chronic ki16425 treatment with inhibition of LPAR improved glucose tolerance and insulin sensitivity in insulin-resistant mice with HFHS diet [23]. In the current study, we found that *Sirt3* deficiency increased serum LPA levels and induced ATX upregulation which facilitated the conversion of LPC to LPA. This was accompanied by increased β cell dedifferentiation in *Sirt3*^f/f;Cre/+ mouse islets and *Sirt3* KD MIN6 cells. These findings supported the notion that SIRT3 expression was essential for suppressing the ATX/LPA pathway for preventing β cell dedifferentiation. We also showed that hyperglycemia suppressed SIRT3 expression in β cells. Once the inhibitory effect of SIRT3 on ATX expression was removed, there was increased secretion of LPA to impair β cell function.

Having discovered that *Sirt3* deficiency induced ATX upregulation, we performed ATX knockdown experiments in mice to confirm whether ATX was the mediator of *Sirt3* deficiency-induced β cell dysfunction. Other researchers had reported increased ATX and LPA expression in HFD-fed mice [23,39]. Similarly, we observed that ATX expression was highly upregulated in islets from *Sirt3*^f/f;Cre/+ mice upon HFD feeding. Knockdown of ATX expression by AAV-*Atx*-shRNA downregulated ATX expression in *Sirt3*^f/f;Cre/+ islets, and decreased circulating ATX and LPA levels. In support of these findings, knockdown of ATX in pancreatic β cells ameliorated HFD-induced β cell dedifferentiation and glucose intolerance found in *Sirt3*^f/f;Cre/+ mice. Similarly, knock-down of ATX in pancreatic β cells relieved the HFD suppression on insulin production in *Sirt3*^f/f;Cre/+ mice. These results supported the notion that ATX was the mediator of *Sirt3* deficiency-induced β cell dysfunction.

In the present study, we observed impaired GSIS of islets from HFD-fed *Sirt3*^f/f;Cre/+ mice although there was no difference between HFD-fed *Sirt3*^f/f and *Sirt3*^f/f;Cre/+ mice in glucose excursion and insulin secretion in response to glucose load. Peterson et al. studied whole-body deletion of SIRT3 (SIRT3 KO) in the C57BL/6 strain [46] and reported that body weight, fasting plasma glucose and insulin levels were similar between STD-fed wild-type (WT) and KO mice. They also found that glucose excursion and insulin secretion in response to either oral or intraperitoneal glucose administration was indistinguishable between both groups of mice fed STD diet. These results were similar to our previous in *Sirt3*^f/f;Cre/+ mice [14,46]. Thus, in the absence of metabolic stress, SIRT3 deficiency was not sufficient to affect glycemic control or insulin secretion. In the aforementioned study, the researchers reported no difference in glucose tolerance between HFHS diet fed SIRT3 KO and WT mice [46]. By contrast, in our previous studies, we found glucose intolerance in SIRT3 KO mice on a 129Sv background and *Sirt3*^f/f;Cre/+ mice in response to HFD feeding [13,14,46]. Of note, the feeding period was lasted for 40 weeks in our previous study compared with the current 12-week study [14,46]. In our study, glucose excursion and insulin secretion in response to glucose load were similar between *Sirt3*^f/f and *Sirt3*^f/f;Cre/+ mice after 6 weeks of HFD feeding according to the AUC of OGTT and insulin secretion, which were similar to the results from Peterson et al. [46]. The impairment in GSIS of islets from HFD-fed *Sirt3*^f/f;Cre/+ mice was similar to our previous studies in islets from HFD-fed SIRT3 KO mice [13,14,46]. This impairment was ameliorated after knocking down ATX expression. Meanwhile, we did not observe any difference in fasting blood glucose, body weight, or food intake among these mice. The lower fasting glucagon level in *Sirt3*^f/f;Cre/+ mice with HFD feeding was consistent with our previous study [14].

In other cellular experiments, MAPKs appeared to be the downstream effectors of LPA pathways [47,48]. In type 1 diabetes, activation of JNK1/2 and JNK could mediate the effects of pro-inflammatory cytokines to cause β cell apoptosis [49]. There was also evidence of JNK activation in diabetic Zucker fatty rats, INS-1 cells under hyperglycemia and human islets from patients with type 2 diabetes [50,51]. Other experimental studies also indicated that JNK1/2 could cause cytoplasmic translocation of PDX1 to suppress insulin gene expression under hyperglycemic and oxidative stress conditions [52]. Our previous study also demonstrated that *Sirt3* deficiency promoted palmitate or H_2O_2-induced JNK phosphorylation in primary islets [13]. Recent work had demonstrated that β cell apoptosis induced by hyperglycemia *in vitro* and *in vivo* might be mediated by p38 MAPK [53]. Consistent with these studies, our results showed that LPA treatment induced phosphorylation of JNK and p38 MAPK in MIN6 cells. Pharmacological inhibition of LPAR not only eliminated the LPA-enhanced phosphorylation of JNK and p38 MAPK but also suppressed the LPA-induced β cell dedifferentiation. In the same vein, both JNK and p38 MAPK inhibitor eliminated LPA-induced β cell dedifferentiation. These results suggested JNK and possibly p38 MAPK might be the downstream effectors during LPA-induced β cell dedifferentiation.

In conclusion, we demonstrated that SIRT3 played a critical role in maintaining functional β cells. In HFD-fed mice, *Sirt3* deficiency in islets induced β cell dysfunction resulting in overt hyperglycaemia. For the first time, we discovered that reduction or absence of *Sirt3* expression upregulated ATX expression with increased production of LPA under metabolic stress. Activation of the ATX/LPA pathway induced β cell dedifferentiation through phosphorylation of JNK/p38 MAPK pathway (Fig. 7). These results add to our current knowledge regarding the regulatory role of *Sirt3* on pancreatic β cell function. In addition to its known local effects on regulating oxidative stress within the cells, our novel data suggested that *Sirt3* might exert a long-range signaling effect by increasing extracellular LPA level through ATX

DUALITY OF INTEREST

AUTHOR CONTRIBUTIONS

J.C.N.C., A.C.K.C., A.P.S.K., H.C., and X.Y.T. contributed to the study concept and design. A.P.S.K., H.C., G.A.R., and X.Y.T. contributed to the data analysis and the writing of the manuscript. H.C., X.M., D.M., H.M.L. and X.C. conducted the in *vitro* and in *vivo* studies. All authors contributed to the critical review of the manuscript and approved the final version of the manuscript. H.C., X.Y.T., and A.P.S.K. are the guarantors of this work and, as such, had full access to all the data in the study and take responsibility for the integrity of the data and the accuracy of the data analysis.

FUNDING

ACKNOWLEDGMENTS

CONFLICT OF INTEREST STATEMENT

APPENDIX A. SUPPLEMENTARY DATA

Supplementary data to this article can be found online at https://doi.org/10.1016/j.molmet.2022.101493.

REFERENCES

[1] Defronzo, R.A., 2009. Banting Lecture. From the triumvirate to the ominous octet: a new paradigm for the treatment of type 2 diabetes mellitus. Diabetes 58(4):773—795.

[2] Kassem, S.A., Ariel, I., Thornton, P.S., Scheimberg, I., Glaser, B., 2000. Beta-cell proliferation and apoptosis in the developing normal human pancreas and in hyperinsulinism of infancy. Diabetes 49(8):1325—1333.

[3] Accili, D., Talchai, S.C., Kim-Muller, J.Y., Cinti, F., Ishida, E., Ordelheide, A.M., et al., 2016. When beta-cells fail: lessons from dedifferentiation. Diabetes, Obesity and Metabolism 18(Suppl 1):117—122.

[4] Talchai, C., Xuan, S., Lin, H.V., Sussel, L., Accili, D., 2012. Pancreatic beta cell dedifferentiation as a mechanism of diabetic beta cell failure. Cell 150(6):1223—1234.

[5] Rutter, G.A., Georgiadou, E., Martinez-Sanchez, A., Pullen, T.J., 2020. Metabolic and functional specialisations of the pancreatic beta cell: gene disallowance, mitochondrial metabolism and intercellular connectivity. Diabetologia 63(10):1990—1998.

[6] Yin, Q., Ni, Q., Wang, Y., Zhang, H., Li, W., Nie, A., et al., 2020. Raptor determines beta-cell identity and plasticity independent of hyperglycemia in mice. Nature Communications 11(1):2538.

[7] Pullen, T.J., Huising, M.O., Rutter, G.A., 2017. Analysis of purified pancreatic islet beta and alpha cell transcriptomes reveals 11beta-hydroxysteroid dehydrogenase (Hsd11b1) as a novel disallowed gene. Frontiers in Genetics 8:41.

[8] Boland, B.B., Brown Jr., C., Boland, M.L., Cann, J., Sulikowski, M., Hansen, G., et al., 2019. Pancreatic beta-cell rest replenishes insulin secretory capacity and attenuates diabetes in an extreme model of obese type 2 diabetes. Diabetes 68(1):131—140.

[9] Gomez-Banoy, N., Guseh, J.S., Li, G., Rubio-Navarro, A., Chen, T., Poirier, B., et al., 2019. Adipsin preserves beta cells in diabetic mice and associates with protection from type 2 diabetes in humans. Nature Medicine 25(11):1739—1747.

[10] Caton, P.W., Richardson, S.J., Kieswich, J., Bugliani, M., Holland, M.L., Marchetti, P., et al., 2013. Sirtuin 3 regulates mouse pancreatic beta cell function and is suppressed in pancreatic islets isolated from human type 2 diabetic patients. Diabetologia 56(5):1068—1077.

[11] Zhang, Y., Zhou, F., Bai, M., Liu, Y., Zhang, L., Zhu, Q., et al., 2019. The pivotal role of protein acetylation in linking glucose and fatty acid metabolism to beta-cell function. Cell Death & Disease 10(2):66.

[12] Kim, M., Lee, J.S., Oh, J.E., Nan, J., Lee, H., Jung, H.S., et al., 2015. SIRT3 overexpression attenuates palmitate-induced pancreatic beta-cell dysfunction. PLoS One 10(4):e0124744.

[13] Zhou, Y., Chung, A.C.K., Fan, R., Lee, H.M., Xu, G., Tomlinson, B., et al., 2017. Sirt3 deficiency increased the vulnerability of pancreatic beta cells to oxidative stress-induced dysfunction. Antioxidants and Redox Signaling 27(13):962—976.

[14] Ming, X., Chung, A.C.K., Mao, D., Cao, H., Fan, B., Wong, W.K.K., et al., 2021. Pancreatic Sirtuin 3 deficiency promotes hepatic steatosis by enhancing 5-hydroxytryptamine synthesis in mice with diet-induced obesity. Diabetes 70(1):119—131.

[15] Stefan, C., Jansen, S., Bollen, M., 2005. NPP-type ectophosphodiesterases: unity in diversity. Trends in Biochemical Sciences 30(10):542—550.

[16] Barbayianni, E., Kaffe, E., Aidinis, V., Kokotos, G., 2015. Autotaxin, a secreted lysophospholipase D, as a promising therapeutic target in chronic inflammation and cancer. Progress in Lipid Research 58:76—96.

[17] Ninou, I., Magkrioti, C., Aidinis, V., 2018. Autotaxin in pathophysiology and pulmonary fibrosis. Frontiers of Medicine 5:180.

[18] Valdes-Rives, S.A., Gonzalez-Arenas, A., 2017. Autotaxin-lysophosphatidic acid: from inflammation to cancer development. Mediators of Inflammation 2017:9173090.

[19] Kaffe, E., Katsifa, A., Xylourgidis, N., Ninou, I., Zannikou, M., Harokopos, V., et al., 2017. Hepatocyte autotaxin expression promotes liver fibrosis and cancer. Hepatology 65(4):1369—1383.

[20] Oikonomou, N., Mouratis, M.A., Tzouvelekis, A., Kaffe, E., Valavanis, C., Vilaras, G., et al., 2012. Pulmonary autotaxin expression contributes to the pathogenesis of pulmonary fibrosis. American Journal of Respiratory Cell and Molecular Biology 47(5):566—574.

[21] Nikitopoulou, I., Oikonomou, N., Karouzakis, E., Sevastou, I., Nikolaidou-Katsaridou, N., Zhao, Z., et al., 2012. Autotaxin expression from synovial

fibroblasts is essential for the pathogenesis of modeled arthritis. Journal of Experimental Medicine 209(5):925—933.

[22] Balood, M., Zahednasab, H., Siroos, B., Mesbah-Namin, S.A., Torbati, S., Harirchian, M.H., 2014. Elevated serum levels of lysophosphatidic acid in patients with multiple sclerosis. Human Immunology 75(5):411—413.

[23] Rancoule, C., Attane, C., Gres, S., Fournel, A., Dusaulcy, R., Bertrand, C., et al., 2013. Lysophosphatidic acid impairs glucose homeostasis and inhibits insulin secretion in high-fat diet obese mice. Diabetologia 56(6):1394—1402.

[24] Scher, M.B., Vaquero, A., Reinberg, D., 2007. SirT3 is a nuclear NAD+-dependent histone deacetylase that translocates to the mitochondria upon cellular stress. Genes & Development 21(8):920—928.

[25] Gao, P., Jiang, Y., Wu, H., Sun, F., Li, Y., He, H., et al., 2020. Inhibition of mitochondrial calcium overload by SIRT3 prevents obesity- or age-related whitening of Brown adipose tissue. Diabetes 69(2):165—180.

[26] Diedisheim, M., Oshima, M., Albagli, O., Huldt, C.W., Ahlstedt, I., Clausen, M., et al., 2018. Modeling human pancreatic beta cell dedifferentiation. Molecular Metabolism 10:74—86.

[27] Yung, Y.C., Stoddard, N.C., Chun, J., 2014. LPA receptor signaling: pharmacology, physiology, and pathophysiology. The Journal of Lipid Research 55(7):1192—1214.

[28] Sidarala, V., Kowluru, A., 2017. The regulatory roles of mitogen-activated protein kinase (MAPK) pathways in health and diabetes: lessons learned from the pancreatic beta-cell. Recent Patents on Endocrine, Metabolic & Immune Drug Discovery 10(2):76—84.

[29] Wang, Z., Zhu, T., Rehman, K.K., Bertera, S., Zhang, J., Chen, C., et al., 2006. Widespread and stable pancreatic gene transfer by adeno-associated virus vectors via different routes. Diabetes 55(4):875—884.

[30] Accili, D., 2018. Insulin action research and the future of diabetes treatment: the 2017 banting medal for scientific achievement lecture. Diabetes 67(9):1701—1709.

[31] Palomer, X., Roman-Azcona, M.S., Pizarro-Delgado, J., Planavila, A., Villarroya, F., Valenzuela-Alcaraz, B., et al., 2020. SIRT3-mediated inhibition of FOS through histone H3 deacetylation prevents cardiac fibrosis and inflammation. Signal Transduction and Targeted Therapy 5:14.

[32] Argaud, D., Boulanger, M.C., Chignon, A., Mkannez, G., Mathieu, P., 2019. Enhancer-mediated enrichment of interacting JMJD3-DDX21 to ENPP2 locus prevents R-loop formation and promotes transcription. Nucleic Acids Research 47(16):8424—8438.

[33] Marchetti, P., Bugliani, M., De Tata, V., Suleiman, M., Marselli, L., 2017. Pancreatic beta cell identity in humans and the role of type 2 diabetes. Frontiers in Cell and Developmental Biology 5:55.

[34] Dhawan, S., Tschen, S.I., Zeng, C., Guo, T., Hebrok, M., Matveyenko, A., et al., 2015. DNA methylation directs functional maturation of pancreatic beta cells. Journal of Clinical Investigation 125(7):2851—2860.

[35] Rutter, G.A., Pullen, T.J., Hodson, D.J., Martinez-Sanchez, A., 2015. Pancreatic beta-cell identity, glucose sensing and the control of insulin secretion. Biochemical Journal 466(2):203—218.

[36] Ishida, E., Kim-Muller, J.Y., Accili, D., 2017. Pair feeding, but not insulin, phloridzin, or rosiglitazone treatment, curtails markers of beta-cell dedifferentiation in db/db mice. Diabetes 66(8):2092—2101.

[37] White, M.G., Shaw, J.A., Taylor, R., 2016. Type 2 diabetes: the pathologic basis of reversible beta-cell dysfunction. Diabetes Care 39(11):2080—2088.

[38] Zhyzhneuskaya, S.V., Al-Mrabeh, A., Peters, C., Barnes, A., Aribisala, B., Hollingsworth, K.G., et al., 2020. Time course of normalization of functional beta-cell capacity in the diabetes remission clinical trial after weight loss in type 2 diabetes. Diabetes Care 43(4):813—820.

[39] Dusaulcy, R., Rancoule, C., Gres, S., Wanecq, E., Colom, A., Guigne, C., et al., 2011. Adipose-specific disruption of autotaxin enhances nutritional fattening and reduces plasma lysophosphatidic acid. The Journal of Lipid Research 52(6):1247—1255.

[40] Nishimura, S., Nagasaki, M., Okudaira, S., Aoki, J., Ohmori, T., Ohkawa, R., et al., 2014. ENPP2 contributes to adipose tissue expansion and insulin resistance in diet-induced obesity. Diabetes 63(12):4154—4164.

[41] Gierse, J., Thorarensen, A., Beltey, K., Bradshaw-Pierce, E., Cortes-Burgos, L., Hall, T., et al., 2010. A novel autotaxin inhibitor reduces lysophosphatidic acid levels in plasma and the site of inflammation. Journal of Pharmacology and Experimental Therapeutics 334(1):310—317.

[42] Rancoule, C., Dusaulcy, R., Treguer, K., Gres, S., Attane, C., Saulnier-Blache, J.S., 2014. Involvement of autotaxin/lysophosphatidic acid signaling in obesity and impaired glucose homeostasis. Biochimie 96:140—143.

[43] Rancoule, C., Dusaulcy, R., Treguer, K., Gres, S., Guigne, C., Quilliot, D., et al., 2012. Depot-specific regulation of autotaxin with obesity in human adipose tissue. Journal of Physiology & Biochemistry 68(4):635—644.

[44] Reeves, V.L., Trybula, J.S., Wills, R.C., Goodpaster, B.H., Dube, J.J., Kienesberger, P.C., et al., 2015. Serum Autotaxin/ENPP2 correlates with insulin resistance in older humans with obesity. Obesity 23(12):2371—2376.

[45] D'souza, K., Nzirorera, C., Cowie, A.M., Varghese, G.P., Trivedi, P., Eichmann, T.O., et al., 2018. Autotaxin-LPA signaling contributes to obesity-induced insulin resistance in muscle and impairs mitochondrial metabolism. The Journal of Lipid Research 59(10):1805—1817.

[46] Peterson, B.S., Campbell, J.E., Ilkayeva, O., Grimsrud, P.A., Hirschey, M.D., Newgard, C.B., 2018. Remodeling of the acetylproteome by SIRT3 manipulation fails to affect insulin secretion or beta cell metabolism in the absence of overnutrition. Cell Reports 24(1):209—223 e6.

[47] Zhang, J., Li, Y., Wang, C., Wang, Y., Zhang, Y., Huang, L., et al., 2020. Lysophosphatidic acid induces apoptosis of PC12 cells through LPA1 receptor/LPA2 receptor/MAPK signaling pathway. Frontiers in Molecular Neuroscience 13:16.

[48] Budnik, L.T., Brunswig-Spickenheier, B., Mukhopadhyay, A.K., 2003. Lysophosphatidic acid signals through mitogen-activated protein kinase-extracellular signal regulated kinase in ovarian theca cells expressing the LPA1/edg2-receptor: involvement of a nonclassical pathway? Molecular Endocrinology 17(8):1593—1606.

[49] Bonny, C., Oberson, A., Negri, S., Sauser, C., Schorderet, D.F., 2001. Cell-permeable peptide inhibitors of JNK: novel blockers of beta-cell death. Diabetes 50(1):77—82.

[50] Syed, I., Jayaram, B., Subasinghe, W., Kowluru, A., 2010. Tiam1/Rac1 signaling pathway mediates palmitate-induced, ceramide-sensitive generation of superoxides and lipid peroxides and the loss of mitochondrial membrane potential in pancreatic beta-cells. Biochemical Pharmacology 80(6):874—883.

[51] Syed, I., Kyathanahalli, C.N., Jayaram, B., Govind, S., Rhodes, C.J., Kowluru, R.A., et al., 2011. Increased phagocyte-like NADPH oxidase and ROS generation in type 2 diabetic ZDF rat and human islets: role of Rac1-JNK1/2 signaling pathway in mitochondrial dysregulation in the diabetic islet. Diabetes 60(11):2843—2852.

[52] Kawamori, D., Kajimoto, Y., Kaneto, H., Umayahara, Y., Fujitani, Y., Miyatsuka, T., et al., 2003. Oxidative stress induces nucleo-cytoplasmic translocation of pancreatic transcription factor PDX-1 through activation of c-Jun NH(2)-terminal kinase. Diabetes 52(12):2896—2904.

[53] Sidarala, V., Veluthakal, R., Syeda, K., Vlaar, C., Newsholme, P., Kowluru, A., 2015. Phagocyte-like NADPH oxidase (Nox2) promotes activation of p38MAPK in pancreatic beta-cells under glucotoxic conditions: evidence for a requisite role of Ras-related C3 botulinum toxin substrate 1 (Rac1). Biochemical Pharmacology 95(4):301—310.